Journal of Engineering and Science Research 6 (6): 59-66, 2022
e-ISSN: 2289-7127

DOI: 10.26666/rmp.jesr.2022.6.5

Papaya Peel-derived Activated Carbon as Potential Adsorbent for Chloramphenicol Compound

Teoh Wei Xin, Noorashrina A Hamid*

[1]School of Chemical Engineering, Engineering Campus, Universiti Sains Malaysia, 14300 Nibong Tebal, Penang, Malaysia
*Corresponding Author: chrina@usm.my

Received: 20 October 2022; Revised: 30 October 2022; Accepted: 25 November 2022; Published: 30 December 2022

Abstract: In this study, papaya peel was converted into papaya peel-derived activated carbon (PPAC) and tested for batch adsorption of CAP. During synthesizing of PPAC, hydrothermal carbonization (HTC) was carried out followed by chemical activation via potassium hydroxide (KOH) and microwave heating to enhance its surface area, porosity, and functional groups. Microwave power for activation process (364-700 W) and initial CAP concentration (5-100 mg/L) were investigated to study the PPAC adsorption capacity and percentage removal. Based on the experimental data, increased microwave power led to an increase in both adsorption capacity and percentage removal until an optimum value. Adsorption capacity also increased when initial CAP concentration increased owing to the higher driving force generated to overcome mass transfer resistance at higher initial CAP concentration. Maximum adsorption capacity of 22.9958 mg/g and maximum percentage removal of 82.40% was achieved. Moreover, the Langmuir isotherm model and pseudo-second-order kinetic model best fitted the data for CAP removal via PPAC. The findings indicated that PPAC was a promising and potential adsorbent in decontaminating CAP from water sources.

Keywords: *Adsorbent, Hydrothermal Carbonization, Papaya Peel*

1. Introduction

The agricultural sector in Malaysia accounted for 8% of the country's gross domestic product (GDP) in 2020 [1]. The annual global agricultural waste production recorded a striking amount of 998 million tons whereas Malaysia contributed 1.2 million tons to the total production [2]. Foo and Hameed (2009) opined that modernity and industrial development not only led to more prosperous and extravagant human lifestyles and habits, but also caused higher generation of municipal solid waste [3]. In the agricultural sector, fruit waste such as fruit peel is not suitable for disposal via conventional burning because of its high moisture content or sanitary landfilling due to the production of leachate from the composted waste [4]. This has prompted research interest in finding a more reliable and promising alternative to minimise or sustain the growing amount of solid waste. One applicable method is converting agricultural waste into economic and efficient activated carbon (AC) to remove pollutants in water sources.

Studies on the removal of antibiotics, particularly chloramphenicol (CAP) using adsorptive materials derived from agricultural waste are scarce. Present work on CAP removal from organic waste-derived AC includes *Typha orientalis*, grape slurry, corn stover, bamboo charcoal and peanut shell [5-9]. Earlier, Hamid and Zulkifli (2021) reported the effect of different carbonisation temperatures (150-200 °C) with a reaction time of 120 minutes on papaya peel-derived hydrochar (PPH) on mass yield, elemental compositions, higher heating value (HHV) and the effectiveness of methylene blue degradation [10]. Nieva *et al.* (2019) also investigated the adsorption capacity of doxycycline using PPH by varying the pH and initial adsorbate concentration [11]. Although Hamid and Zulkifli (2021) had investigated the removal of methylene blue using PPH, no literature presents the removal of CAP using AC prepared from papaya peel despite its abundance and availability in Malaysia.

Corresponding Author: Anas Abdul Rahman, Mechanical Engineering Program, Faculty of Mechanical Engineering Technology, Universiti Malaysia Perlis, Pauh Putra Main Campus, 02600 Arau, Perlis, Malaysia, anasrahman@unimap.edu.my

Moreover, as mentioned previously, the physiochemical properties of AC depend on the type of feedstock and the processing condition of both HTC and chemical activation. However, as recent work mainly focused on developing hydrochar from various carbonaceous sources and enhancing adsorption performance based on different carbonisation and activation conditions such as different carbonisation temperature, retention time and impregnation ratio, an in-depth discussion on microwave heating technique and its performance enhancement on the hydrochar-derived AC are limited [12]. Furthermore, as the conventional heating technique is still the most widespread and known method to prepare an AC, there is no present study on the usage of microwave-irradiated biomass AC in CAP removal.

Therefore, this work intends to study the effect of chemical activation on the characterisation of PPAC by examining the differences between PPH and PPAC. Next, the adsorption capacity and percentage removal of CAP from PPAC activated from different microwave powers are inspected. Furthermore, change in initial concentrations of CAP is also investigated further to maximise the adsorption capacity and removal efficiency of PPAC.

2. Materials and Methods

The ripened papaya fruit peel was washed with distilled water to remove dirt from its surface prior to cutting into smaller pieces and dried in an oven for 18 h at 120 ºC. Next, the small papaya peel pieces were ground using a blender to powder them before being filtered using an 80-mesh sieve to obtain uniformly-sized powder.

2.1. Hydrothermal Carbonisation of Hydrochar

About 15 g papaya peel powder was mixed with 150 mL distilled water and poured into a 200 mL stainless steel hydrothermal reactor. The hydrothermal reactor was then heated in an oven for 2 h at 150 ºC [10]. After cooling to room temperature, the content was filtered and washed repeatedly with distilled water to separate the solid and liquid products. The washed solid hydrochar was collected in a ceramic evaporating dish and further dried using an oven at 120 ºC for 18 h [10]. 2 g of solid hydrochar was put aside in a container labelled PPH for the characterization process.

2.2. Chemical Activation of Hydrochar

To produce an alkaline-modified AC, PPH powder was impregnated with 1.5 M potassium hydroxide (KOH) solution at room temperature for 6 h at an impregnation ratio of 1.25:1 (KOH:AC). The treated mixture was then dried in an oven for 18 h at 120 ºC. After drying and cooling, the alkaline-modified powder was heated in a microwave for 6 min at 364 W under continuous nitrogen (N_2) flow to form PPAC. After heating, the AC produced was washed with 0.5 M hydrochloric acid (HCl) followed by hot distilled water to remove the residual KOH until the pH of the solution fell between 6-6.5. The alkaline-modified AC was finally dried for 18 h at 120 ºC. The dried powder was kept in a container labelled PPAC (364 W).

The experiment was repeated using different microwave powers of 511 W, 616 W and 700 W. The products were kept in containers labelled PPAC (511 W), PPAC (616 W) and PPAC (700 W) respectively.

2.3. Characterisation of Hydrochar

Two different samples were collected for the characterization process: papaya peel-derived hydrochar (PPH) and papaya peel-derived activated carbon (PPAC) using a microwave power of 511 W. Field Emission Scanning Electron Microscopy (SEM) (Quanta 450, FEI) was used to evaluate the morphological characterization of papaya peel powder samples. Meanwhile, Fourier Transform Infrared Spectroscopy (FTIR) spectrometer (IRPrestige-21, Shimadzu) was used to assess the samples' surface functional groups. To analyze the gas adsorption data and determine the specific surface area of each sample, the Brunauer, Emmett, and Teller (BET) surface area apparatus (ASAP 2020, Micromeritics) was utilised.

2.4. Batch Adsorption of Chloramphenicol

0.4 g of PPAC activated via 364 W microwave power was mixed with 150 mL CAP solution of concentration 5 mg/L in a 250 mL conical flask. The mixture was agitated using a water bath shaker at 100 rpm and room temperature for 24 h. 4.5 mL of each sample was withdrawn at fixed intervals and filtered through a 0.45 μm membrane filter. This step lasted for 24 h. The collected samples in cuvettes were then inserted into a UV-Vis spectrophotometer to determine their residual concentrations and absorbances.

The adsorption capacity and removal capacity of CAP using AC were then computed based on the equations below:

$$Q_t = \frac{(C_o - C_e)V}{W} \quad (1)$$

where,

Q_t = Adsorption capacity at time t (mg/g)

C_o = Initial concentration of adsorbate (mg/L)

$$\text{Removal Efficiency (\%)} = \frac{(C_o - C_e)}{C_o} \times 100\% \quad (2)$$

C_e = Concentration of adsorbate at equilibrium (mg/L)

V = Volume of solution (L)

W = Mass of adsorbent (g)

To assess the effect of microwave power, the experiment was done using PPAC of different microwave powers at 511 W, 616 W and 700 W. Next, the second experiment on the effect of initial CAP concentration was conducted using different concentrations of CAP at 10 mg/L, 30 mg/L, 50 mg/L and 100 mg/L. In this parameter study,

510 W microwave power of PPAC was selected based on the best adsorption capacity and percentage removal values from the previous microwave power study.

The experimental results on the effect of initial CAP concentration were then fitted to the linearised forms of adsorption isotherms, including Langmuir, Freundlich and Temkin isotherms. Kinetic studies were also done by fitting the data to the kinetic models, namely pseudo-first-order and pseudo-second-order models.

3. Results and Discussion

3.1 Characterisation of Papaya Peel-Derived Hydrochar and Activated Carbon

3.1.1 Scanning Electron Microscopy (SEM) Analysis

Micrograph images obtained from SEM of the PPH before and after activation at magnifications of 500x and 3000x were shown in Figure 1. The surface morphology of PPH showed stone-like rough structures with uneven surfaces and no clear and defined pore spaces Figure 1 (a). The closed porosity contributed to very limited intraparticle infusibility as the internal surfaces were inaccessible [8].

On the other hand, in Figure 1(b), the morphology of PPAC appeared as a cluster of particulates with distinct and irregular cavities or open pore spaces of multiple sizes. Irregular pore structures are present in all directions. Chemical activation transformed the hydrochar into AC by generating well-defined micropores and mesopores [13]. The cavities observed resulted from the evaporation of KOH activating agent during thermal treatment via microwave, removing the traces of KOH and leaving tiny voids on the adsorbent surfaces [14]. Similarly, large morphological transformation was also observed between pineapple char and chemically activated pineapple AC where the initial pineapple char had a constricted and dense surface whereas its AC demonstrated well-pronounced and highly porous structures as reported by Foo and Hameed [15]. Thus, chemical activation and the subsequent microwave irradiation process were proven to induce porosity in the surface morphology of biomass.

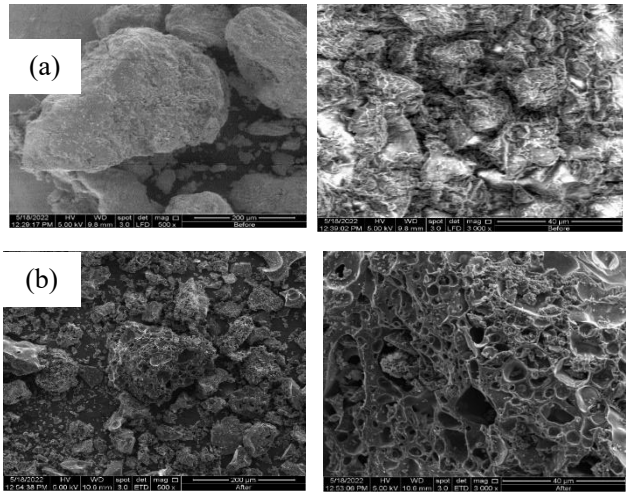

Figure 1. Scanning Electron Micrographs of (a) PPH and (b) PPAC at Magnifications of 500x and 3000x, respectively

3.1.2 BET Analysis

As the application of AC was highly subjected to the porosity of material, activation process served the purpose of intensifying the surface area and pore structure of hydrochar. The data collected from N_2 adsorption/desorption isotherms were arranged in Table 1. The BET surface area was determined using the Brunauer-Emmett-Teller (BET) equation whereas micropore volume, micropore surface area and external surface area were predicted using the t-Plot method. It was noticeable that the BET surface area, S_{BET} of PPAC which was chemically-activated with KOH and microwave-heated was tremendously larger than its inactivated counterpart with values of 0.1200 m^2/g and 660.7779 m^2/g respectively. This signified the importance of the activation process as adsorbents with a larger SBET usually indicated better adsorption capacity [17]. The widened and developed pore structures on the AC adsorbent surfaces attract absorbates with similar or smaller dimension to adhere to them through pore effects such as pore filling for similarly sized adsorbate molecules and size exclusion for molecules with smaller pore diameter [6]. This justification complied with the SEM analysis results in the previous section where PPAC had clear and evident increase in pore size compared to PPHs.

Table 1. Physical Properties of PPH and PPAC

Sample/Description	PPH	PPAC
BET Surface Area (m^2/g)	0.1200	660.7779
Langmuir Surface Area (m^2/g)	0.1303	900.9353
t-Plot Micropore Volume (cm^3/g)	-	0.2833
t-Plot Micropore Area (m^2/g)	-	585.2372
t-Plot External Surface Area (m^2/g)	-	75.5407

3.1.3. FTIR Analysis

FTIR analysis dissected the chemical functional groups present in the samples for a rudimentary insight into the mechanism underlying CAP's adsorption process. Based on the FTIR spectra of PPH and PPAC displayed in Figure 2, both samples recorded the spectra pattern in the range of 400-4000 cm^{-1}. PPH detected absorption bands at 619.15, 1053.13, 1417.68, 1651.07, 2424.52, 2912.51 and 3410.15 cm^{-1} corresponding to alkyne C-H bend, primary alcohol C-O stretch, methyl and methylene C-H stretch, in-plane O-H blend, alkenyl C-C stretch, alkyne C-C stretch and N-H stretch. At the same time, PPAC detected similar absorption bands at 621.08, 1028.06, 1527.62, 2330.01, 3593.38 and 3720.69 cm^{-1}. The elimination of 1651.07 and 2912.51 cm^{-1} peaks indicated that the deformation or decomposition of functional groups and the release of volatile matters occurred during microwave heating [8,15].

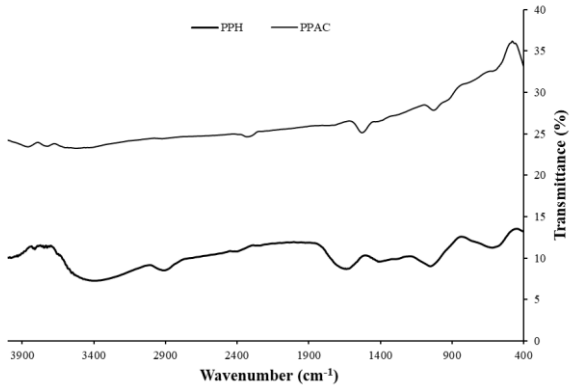

Figure 2. FTIR Spectra for PPH and PPAC

3.2. Effect of Microwave Power on Papaya Peel-Derived Activated Carbon

Adsorption of CAP by PPAC was demonstrated by subjecting 0.4 g of AC produced from varying microwave powers of 364 W, 511 W, 616 W and 700 W to 150 mL 5 mg/L CAP at room temperature of 30 ºC. The effect of activation microwave power on the adsorption capacity and percentage removal of CAP were illustrated in Figure 3 and 4, respectively.

Figure 3 showed that the adsorption capacity for each microwave power increased sharply from 0 min to 100 min. Beyond 100 min, the increments slowed down and the adsorption capacities for all curves increased gradually at a lower rate. This was due to the abundance of available adsorption sites at the initial stage of adsorption process. As time progressed, more active sites were occupied, and fewer vacant sites were present [8]. Diffusion resistance and the repulsive forces between the CAP molecules adsorbed on surface of AC and the CAP molecules to be adsorbed increased, thus slowing down the adsorption pace [6]. Gradually, adsorption equilibrium was achieved at 1440 min or 24 h.

Besides, Figure 4 outlined the relationship between percentage removal of CAP and time for several microwave power levels. Like the former plot, the increase of removal percentage in the first 100 min was rapid, followed by a relatively slower rate of removal of CAP in the next minutes until equilibrium time at 1440 min or 24 h.

The overall trends observed that both adsorption capacities and percentage removal of chemically AC increased in the order of 364 W, 700 W, 616 W, 511 W. The adsorption capacity increased with increased microwave power from 364 W to 511 W. This was attributed to the less developed pore structure at lower microwave power. Increased microwave power enhanced the expansion of carbon structure and the opening of surface pores, enabling more active sites to be formed on the adsorbent surface. Internal and volumetric heating occurred at the same time, contributing to a better pore structure development and enhancement in adsorption uptake capacity of CAP [17]. Nonetheless, beyond 511 W, its adsorption capacity decreased with a further increase in microwave power. This trend was in line with previous work [14-16]. It is obvious that the elevation of microwave power past its optimum level induced fiercer reaction and rapid dehydration, leading to greater burn off in carbon weight and subsequently lower adsorption performance [16-17]. Also, rupture of pore structure occurred due to over-gasification and excessive microwave energy at elevated power.

From the experiment, 511 W microwave power was the optimum power level for activation of KOH-induced PPAC, with the highest adsorption capacity of 1.7978 mg/g and the highest removal percentage of 82.40 %. The removal percentage had an almost similar value to the study from Li *et al.* [6] that recorded an 83.40% removal percentage of CAP using *Typha orientalis*.

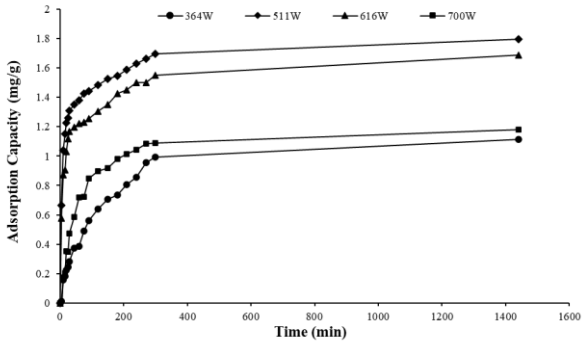

Figure 3. Adsorption Capacity of PPAC on CAP at different Microwave Powers

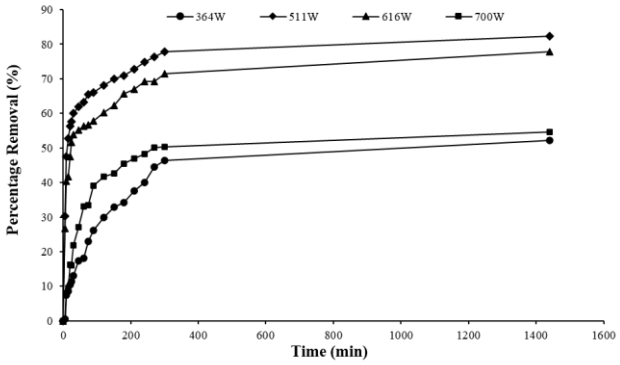

Figure 4. Percentage Removal of PPAC on CAP at different Microwave Powers

3.3 Effect of Initial Chloramphenicol Concentration on Papaya Peel-Derived Activated Carbon

Using the best microwave power for activation and adsorption performance of PPAC which is 511 W from the previous section, batch adsorption experiments of multiple initial CAP concentrations at 5 mg/L, 10 mg/L, 30 mg/L, 50 mg/L and 100 mg/L were performed at room temperature of 30 ^{o}C. 0.4 g of PPAC is agitated with 150 mL of CAP. The effect of initial CAP concentration on the adsorption capacity and percentage removal of CAP were depicted in Figure 5 and 6, correspondingly. Adsorption capacity was noticed to also increase drastically at first, followed by a gradual increase until an equilibrium point was reached where AC was unable to uptake more CAP, which is in similar manner to Figure 3. However, it was observed that the equilibrium points were not reached for 50 mg/L and 100 mg/L CAP solutions even after 24 h. It is also showed that CAP's adsorption capacity increased with the rise in initial CAP concentration. Chitongo et al. [8] deduced that as initial CAP concentration increased, more driving force was created to overcome the mass transfer resistance between CAP in the bulk aqueous solution and CAP adhered to the adsorbent surface. As a result, higher adsorption capacity was recorded at higher initial CAP concentration as more driving force was generated for mass transfer between the aqueous and solid phases, allowing enhanced collision between CAP molecules and the active sites and thus, diffusion efficiency became higher [6-7]. In the present study, the equilibrium adsorption capacity, Qe increased from 1.7978 mg/g to 22.9958 mg/g when the CAP initial concentration increased from 5 mg/L to 100 mg/L. However, it was worth noting that the slope of adsorption capacity became steeper as the initial CAP concentration increased. Furthermore, as CAP initial concentration increased, longer time was needed to achieve equilibrium.

Nevertheless, from Figure 6, an inverse relationship between removal percentage capacity and initial CAP concentration was established. When the initial concentration of CAP increased, its removal percentage decreased. This finding explained that as an adsorbent has a finite number of active sites, the decline in adsorption efficiency was attributed to the achievement of saturation due to the occupation of adsorption sites at high antibiotic concentrations. When the mass of AC remained constant, but the concentration of CAP increased, the limited availability of vacant sites became saturated earlier and more difficult to cater to higher moles of CAP, leading to decreased effectiveness [8,18].

The highest adsorption capacity of 22.9958 mg/g was achieved at the initial CAP concentration of 100 mg/L. Inversely, the lowest removal percentage of 62.86 % was obtained in the experiment of 100 mg/L initial CAP concentration after 24 h. The experimental results showed that the CAP adsorption activities in aqueous solutions were favoured by lower initial CAP concentrations as it had higher percentage removal of antibiotics.

3.4 Adsorption Isotherm

The estimated constant value for each isotherm model reported were summarised in Table 2. In order to determine the accuracy of model fitting statistically, correlation coefficient, R^2 was employed as the comparison criterion. Higher R^2 value accounted for smaller differences between the experimental data and the fitted linear regression line. From the graph, the R^2 in order of Langmuir, Freundlich and Temkin isotherms were 0.9976, 0.9808 and 0.9645 respectively. Langmuir model described the adsorption data most precisely by comparison as it had $R^2 \geq 0.99$.

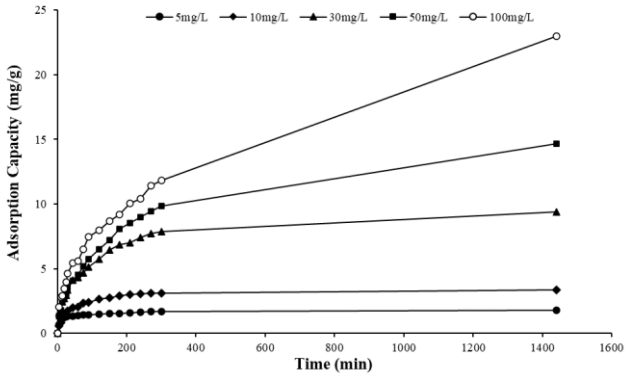

Figure 5. Adsorption Capacity of PPAC on CAP at different Initial CAP Concentrations

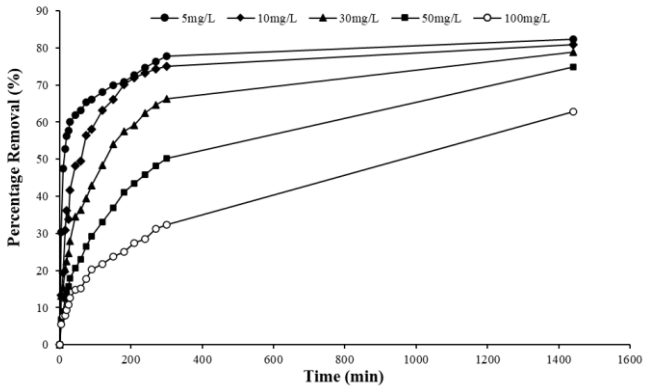

Figure 6. Percentage Removal of PPAC on CAP at different Initial CAP Concentrations

The experimental data was best fitted to Langmuir model, followed by Freundlich model and finally Temkin model. Using Langmuir isotherm, the maximum monolayer adsorption capacity, Q_m of PPAC was 35.3357 mg/g whereas the Langmuir isotherm constant, K_L is 0.0523 L/mg. The separation factor, R_L for the adsorption process onto PPAC was within the range of $0.1384 \leq R_L \leq 0.4422$, showing that the adsorption was efficient as it lied between the favourable range of $0 \leq R_L \leq 1$ [19]. On top of that, as the value of 1/n described the adsorption intensity or surface heterogeneity, the value of 0.7342 ($1/n \leq 1$) obtained suggested that CAP is favourably physically adsorbed on PPAC.

Langmuir isotherm in this case inferred that monolayer adsorbate, which is CAP formed on the outer surface of PPAC. No further adsorption occurred afterwards as the surface exhibited finite number of active sites. Uniform energy of adsorption was also assumed in this isotherm model [15].

Table 2. Adsorption Isotherm Parameters of Langmuir, Freundlich and Temkin Models for Adsorption of CAP on PPAC

Parameter	Value
Langmuir Isotherm	
K_L (L/mg)	0.0523
Q_m (mg/g)	35.3357
R_L	0.1384-0.4422
R^2	0.9976
Freundlich Isotherm	
K_F ((mg/g)·(L/mg)$^{1/n}$)	1.9619
n_F	1.3620
R^2	0.9808
Temkin Isotherm	
K_T (L/mg)	0.9712
B (J/mol)	6.0059
b_T (kJ/mol)	419.4445
R^2	0.9645

3.5 Adsorption Kinetics

The experimental and calculated adsorption capacities, rate constants and correlation coefficients were tabulated in Table 3. Considering the statistical measures, the correlation coefficient, R^2 of pseudo-first order and pseudo-second-order kinetic models for 5 mg/L CAP samples were in the range of 0.85-0.98 and 0.91-0.99 respectively, deeming the pseudo-second-order kinetic model better described the adsorption kinetics of CAP on PPAC.

This confirmed that the rate-limiting step was chemisorption which occurred by valence forces via electron exchange between PPAC and CAP. It was reported that the amount of adsorbate adsorbed at equilibrium, $Q_{e,cal}$ followed an increasing trend when the initial CAP concentration was increased. Increase of $Q_{e,cal}$ reflected that higher initial CAP concentrations provided a stronger driving force to break through the mass transfer-resistance barrier between the solid and aqueous phases during adsorption [7].

Table 3. Adsorption Kinetics Parameters of Pseudo-first-order and Pseudo-second-order Kinetic Models for Adsorption of CAP on PPAC

Parameter	Value				
	C_o (mg/L)				
	5	10	30	50	100
$Q_{e,exp}$ (mg/g)	1.7978	3.3641	9.3855	14.6850	22.9958
Pseudo-first-order Kinetic Model					
	C_o (mg/L)				
	5	10	30	50	100
$Q_{e,cal}$ (mg/g)	0.7762	2.3345	7.5338	12.8597	20.2509
k_1 (min^{-1})	0.0030	0.0036	0.0025	0.0015	0.0009
R^2	0.8595	0.9624	0.9815	0.9806	0.9537
Pseudo-second-order Kinetic Model					
	C_o (mg/L)				
	5	10	30	50	100
$Q_{e,cal}$ (mg/g)	1.8083	3.4282	9.6712	15.4321	24.0964
k_2 (min^{-1})	0.0.32	0.0097	0.0017	0.0005	0.0002
R^2	0.9992	0.9993	0.9956	0.9762	0.9142

3.6 Comparison of Papaya Peel-Derived Activated Carbon with Literature

Current work presented raw papaya peel carbonised via HTC to produce PPH and subsequently impregnated using KOH and thermally treated with microwave to produce PPAC. Table 4 collected the BET surface area of different biomass AC reported in other literature.

By comparison, PPAC had an S_{BET} of 660.7779 m^2/g, which was still average as it had larger S_{BET} than bamboo charcoal, oat hull and cotton stalk ACs [5,15,20]. Larger S_{BET} usually indicated better uptake capability of adsorbate onto the adsorbent surface. This result proved the practicability of producing AC from papaya peels to function in adsorbing contaminants such as methylene blue and CAP. It also had almost similar S_{BET} as pineapple peel [15]. From the comparison of different activating agents and heating temperatures and retention times, there was no noticeable trend indicating that increasing heating temperatures or durations give rise to larger S_{BET}. The optimal modification temperature and duration were highly dependent on the types

and the morphological structures of the raw material. However, the operating conditions were still not completely optimised as there were more parameters affecting the porosity and functionalisation of PPAC beyond the content investigated in this work. So, this proved that PPAC had even higher potential in CAP adsorption than it had now when other parameters such as carbonisation temperatures, activation temperatures, types of activating agent and impregnation ratio were investigated and taken into consideration.

Table 4. Comparison of BET Surface Area of Various AC

Raw Material	Activating Agent	Thermal Treatment	BET Surface Area (m^2/g)	Reference
Bamboo Charcoal	H_2SO_4	-	<1	[5]
Typha orientalis	H_3PO_4	Conventional Heating, 450 °C, 1 h	795	[6]
Corn Stover	-	Physical, 600 °C, 2 h	962	[7]
Cotton Stalk	KOH	Microwave, 680 W, 8 min	729	[14]
Cotton Stalk	K_2CO_3	Microwave, 660 W, 10 min	621	[14]
Pineapple Peel	K_2CO_3	Microwave, 600 W, 6 min	680	[15]
Oat Hull	H_3PO_4	Microwave, 700 W, 9 min	461	[20]
Papaya Peel	KOH	Microwave, 511 W, 6 min	661	Present Work

Apart from that, Table 5 summarised the comparison of maximum capacity, type of isotherm model and kinetics model of multiple precursors from various works. As the current work on adsorption of CAP using biomass-derived AC were still scarce, only a few Q_m on CAP from these AC were reported by previous researchers. In contrast with the other biomass-derived AC, papaya peel was still weighed up to its practicability and reusability with a maximum adsorption capacity of 22.9958 mg/g and maximum percentage removal of 82.40%. It had relatively higher Q_m than grape slurry and bamboo charcoal on CAP removal. Except *Typha orientalis* AC, all AC stated in Table 5 correlated to Langmuir isotherm, signifiying that the adsorption process represented homogeneous monolayer adsorption [5,8]. On top of that, all experiment data followed pseudo-second-order kinetic model which described chemisorption as the rate-controlling process for CAP adsorption.

Table 5. Comparison of Adsorption Capacities of Various AC for CAP

Raw Material	Activa t-ing Agent	Maximum Adsorption Capacity (mg/g)	Isotherm Model	Kinetics Model	Reference
Bamboo Charcoal	NaOH	2.8	Langmuir	-	[5]
Typha orientali s	H_3PO_4	137.1	Freundlich	Pseudo-second-order	[6]
Corn Stover	-	32.3	Langmuir	Pseudo-second-order	[7]
Grape Slurry	KOH	2.6	Langmuir	Pseudo-second-order	[8]
Papaya Peel	KOH	23.0	Langmuir	Pseudo-second-order	Present Work

4. Conclusion

PPAC was successfully produced via hydrothermal carbonization followed by chemical activation. SEM results showed formation of well-defined pores on the adsorbent surfaces in PPAC while BET surface area increased gradually from 0.0012 m^2/g (PPH) to 660.7779 m^2/g (PPAC) due to the porosity formation. A lower percentage removal of CAP was recorded with increasing initial CAP concentration. The CAP uptake and percentage removal of 5 mg/L CAP were at its highest of 1.7978 mg/g and 82.40% when 511 W microwave power was employed in the chemical activation process to produce PPAC. Maximum adsorption capacity with a value of 22.9958 mg/g was attained at 100 mg/L CAP solution with the least percentage removal of 62.86%. On the contrary, maximum percentage removal was reached at 82.40% when 5 mg/L CAP solution was used. Langmuir isotherm model contributed to a better fit indicating that monolayer adsorption occured at the adsorbent surface. Furthermore, pseudo-second-order kinetic model provided a better fit in the adsorption of CAP onto PPAC, confirming that chemisorption was the rate-limiting step in the process.

Acknowledgements

Author is thankful to the Universiti Sains Malaysia for the opportunities to conduct this research.

5.0 References

[1] Online Available at: https://www.trade.gov/country-commercial-guides/malaysia-agricultural-sector (Accessed: January 1, 2022).

[2] Online Available at: https://ap.fftc.org.tw/article/1381 (Accessed: July 7, 2022).

[3] K.Y. Foo, and B.H. Hameed, An overview of landfill leachate treatment via activated carbon adsorption process, Journal of Hazardous Materials, pp. 54–60. 2009, Available at: https://doi.org/10.1016/j.jhazmat.2009.06.038.

[4] P. Kantakanit, N. Tippayawong, S. Koonaphapdeelert, A. Pattiya, Hydrochar Generation from Hydrothermal Carbonization of Organic Wastes, in IOP Conference Series: Earth and Environmental Science. Institute of Physics Publishing, 2018. Available at: https://doi.org/10.1088/1755-1315/159/1/012001.

[5] Y. Fan, B. Wang, S. Yuan, X. Wu, J. Chen, L. Wang, Adsorptive removal of chloramphenicol from wastewater by NaOH modified bamboo charcoal, Bioresource Technology, 101(19), pp. 7661–7664, 2010. Available at: https://doi.org/10.1016/j.biortech.2010.04.046.

[6] Y. Li, J. Zhang, H. Liu, Removal of chloramphenicol from aqueous solution using low-cost activated carbon prepared from Typha orientalis, Water (Switzerland), 10(4), 2018. Available at: https://doi.org/10.3390/w10040351.

[7] X. Cheng, C. Zheng, Q. Liu, J. Liu, Adsorption of Furazolidone, D-Cycloserine, and Chloramphenicol on Granular Activated Carbon Made from Corn Stover, Journal of Environmental Engineering, 145(7), p. 04019038, 2019. Available at: https://doi.org/10.1061/(asce)ee.1943-7870.0001546.

[8] R. Chitongo, B. O. Opeolu, O. S. Olatunji, Abatement of Amoxicillin, Ampicillin, and Chloramphenicol From Aqueous Solutions Using Activated Carbon Prepared From Grape Slurry, Clean - Soil, Air, Water, 47(2), 2019. Available at: https://doi.org/10.1002/clen.201800077.

[9] J. Yang, G. Ji, Y. Gao, W. Fu, M. Irfan, L. Mu, Y. Zhi, A. Li, High-yield and high-performance porous biochar produced from pyrolysis of peanut shell with low-dose ammonium polyphosphate for chloramphenicol adsorption, Journal of Cleaner Production, 264, pp. 121516, 2020. Available at: https://doi.org/10.1016/j.jclepro.2020.121516.

[10] N. A. A. Hamid, N. Z. Zulkifli, Papaya peels as source of hydro char via hydrothermal carbonization, in IOP Conference Series: Earth and Environmental Science. IOP Publishing Ltd, 2021. Available at: https://doi.org/10.1088/1755-1315/765/1/012001.

[11] A. D. Nieva, R. J. Q. Buenafe, L. M. S. Orense, J. M. R. Trinida, Biosorption of doxycycline using Carica papaya L. peels," in IOP Conference Series: Earth and Environmental Science. Institute of Physics Publishing, 2019. Available at: https://doi.org/10.1088/1755-1315/344/1/012010.

[12] Y. L. Chávez and Galiano, Landfill leachate treatment using activated carbon obtained from coffee waste, Engenharia Sanitaria e Ambiental, 24(4), pp. 833–842, 2019. Available at: https://doi.org/10.1590/s1413-41522019178655.

[13] R. Zhang, Z. Zhou, A. Xie, J. Dai, J. Cui, J. Lang, M. Wei, X. Dai, C. Li, Y, Yan, Preparation of hierarchical porous carbons from sodium carboxymethyl cellulose via halloysite template strategy coupled with KOH-activation for efficient removal of chloramphenicol, Journal of the Taiwan Institute of Chemical Engineers, 80, pp. 424–433, 2017. Available at: https://doi.org/10.1016/j.jtice.2017.07.032.

[14] H. Deng, G. Li, H. Yang, J. Tang, J. Tang, Preparation of activated carbons from cotton stalk by microwave assisted KOH and K2CO3 activation, Chemical Engineering Journal, 163(3), pp. 373–381, 2010. Available at: https://doi.org/10.1016/j.cej.2010.08.019.

[15] K. Y. Foo, B. H. Hameed, Porous structure and adsorptive properties of pineapple peel based activated carbons prepared via microwave assisted KOH and K2CO 3 activation, Microporous and Mesoporous Materials, 148(1), pp. 191–195, 2012a Available at: https://doi.org/10.1016/j.micromeso.2011.08.005.

[16] A. M. Abioye, F. N. Ani, Advancement in the production of activated carbon from biomass using microwave heating, Jurnal Teknologi, 79(3), pp. 79–88, 2017. Available at: https://doi.org/10.11113/jt.v79.7249.

[17] A. Vimalkumar, J. Thilagan, K. Rajasekaran, C. Raja, M. Flora, Preparation of activated carbon from mixed peels of fruits with chemical activation (K 2 CO 3)-application in adsorptive removal of methylene blue from aqueous solution, Int. J. Environment and Waste Management, 2018.

[18] B. O. Fagbayigbo, B. O. Opeolu, O. S. Fatoki, Adsorption of perfluorooctanoic acid (PFOA) and perfluorooctane sulfonate (PFOS) from water using leaf biomass (Vitis vinifera) in a fixed-bed column study, Journal of Environmental Health Science and Engineering, 18(1), pp. 221–233, 2020. Available at: https://doi.org/10.1007/s40201-020-00456-1.

[19] J. Wang, X. Guo, Adsorption isotherm models: Classification, physical meaning, application and solving method, Chemosphere. Elsevier Ltd, 2020a. Available at: https://doi.org/10.1016/j.chemosphere.2020.127279.

[20] Z. Movasaghi, B. Yan, C. Niu, Adsorption of ciprofloxacin from water by pretreated oat hulls: Equilibrium, kinetic, and thermodynamic studies, Industrial Crops and Products, 127, pp. 237–250, 2019. Available at: https://doi.org/10.1016/j.indcrop.2018.10.051.